



Article

# Structural Features and Phylogenetic Implications of Crinoid Echinoderms Based on Thirteen Novel Mitochondrial Genomes

Qinzeng Xu <sup>1,2,\*</sup> , Min Lu <sup>1</sup>, Yuyao Sun <sup>1,2</sup>, Zhong Li <sup>1,3</sup>, Yixuan Li <sup>4</sup>, Yue Dong <sup>1,3</sup>, Xuying Hu <sup>1</sup>, Qian Zhang <sup>1</sup>, Bing Liu <sup>1</sup>  and Xuebao He <sup>5,\*</sup>

- <sup>1</sup> Key Laboratory of Marine Eco-Environmental Science and Technology, First Institute of Oceanography, Ministry of Natural Resources, Qingdao 266061, China; lumin928105@163.com (M.L.); sy18335462304@163.com (Y.S.); lizhong@fio.org.cn (Z.L.); dongyue@fio.org.cn (Y.D.); huxuying@fio.org.cn (X.H.); zhangqian26@fio.org.cn (Q.Z.); liub@fio.org.cn (B.L.)
- <sup>2</sup> Laboratory for Marine Ecology and Environmental Science, Qingdao Marine Science and Technology Center, Qingdao 266237, China
- <sup>3</sup> College of Environmental Science and Engineering, Ocean University of China, Qingdao 266100, China
- <sup>4</sup> Department of Biology, Hong Kong Baptist University, Kowloon 999077, Hong Kong SAR, China; liyixuan176@163.com
- <sup>5</sup> Laboratory of Marine Biodiversity, Third Institute of Oceanography, Ministry of Natural Resources, Xiamen 361005, China
- \* Correspondence: xqz08@163.com (Q.X.); hexuebao@tio.org.cn (X.H.)

**Abstract:** Crinoids, as integral echinoderms, play a crucial ecological role in benthic communities, serving as significant indicators reflecting the health of marine ecosystems. However, the phylogenetic relationships within crinoids are unclear. More molecular data can help to facilitate biodiversity assessment and elucidate evolutionary relationships by the phylogenetic tree. In this study, 13 complete mitochondrial genomes of the Crinoidea class were sequenced, annotated, and compared with other same class species available on NCBI. The results reveal five different gene order patterns among these mitochondrial genomes, indicating that crinoids have undergone gene rearrangements during evolution. The complete mitochondrial genome length of crinoids ranges from 15,772 bp to 16,850 bp. High A + T content, ranging from 64.5% to 74.2%, was observed. Additionally, our analysis of protein-coding genes highlights a preference for A + T nucleotides, along with specific start and stop codon usage, offering insights into codon bias and its implications for protein synthesis and function. The phylogenetic topology shows that the stalkless crinoid and stalked crinoid are distinct, and the phylogenetic trees generated based on maximum likelihood and Bayesian inference are almost identical at the family and order topology levels. The phylogenetic relationships of each family were fully clarified in four orders. A total of eleven positive selection sites were detected within six genes: *cytb*, *nad2*, *nad3*, *nad4*, *nad4L* and *nad5*. This study reveals the phylogenetic relationships of crinoid species, the mitochondrial gene differences, and the selective pressure on the evolution of stalked crinoids. This study significantly enhanced the crinoid mitochondrial genome database and contributed to a better understanding of the phylogenetic relationships among crinoid echinoderms.

**Keywords:** crinoids; echinoderm; mitochondrial genome; mitochondrial structure character



**Citation:** Xu, Q.; Lu, M.; Sun, Y.; Li, Z.; Li, Y.; Dong, Y.; Hu, X.; Zhang, Q.; Liu, B.; He, X. Structural Features and Phylogenetic Implications of Crinoid Echinoderms Based on Thirteen Novel Mitochondrial Genomes. *J. Mar. Sci. Eng.* **2024**, *12*, 361. <https://doi.org/10.3390/jmse12030361>

Academic Editor: Azizur Rahman

Received: 22 December 2023

Revised: 28 January 2024

Accepted: 15 February 2024

Published: 20 February 2024



**Copyright:** © 2024 by the authors. Licensee MDPI, Basel, Switzerland. This article is an open access article distributed under the terms and conditions of the Creative Commons Attribution (CC BY) license (<https://creativecommons.org/licenses/by/4.0/>).

## 1. Introduction

Crinoids have been present in oceanic ecosystems for more than 500 million years, displaying a remarkable range of diversity across various marine environments, from tropical to polar seas and from intertidal zones to the depths of the ocean [1,2]. Based on their attachment type, crinoids are categorized into two main types: stalked crinoids and stalkless crinoids. Stalked crinoids [3] have a stalk throughout life and adopt a fixed way of life. Their body shape resembles a plant with three distinct sections: root, stem, and crown. They primarily inhabit the deep seas. Stalkless crinoids [4] (order: Comatulida) are stationary as adults but can freely move across the seafloor. Their varied shapes reflect

adaptations to different habitats and niches. Most of them inhabit coastal shallow sea rocks or hard bottoms [5].

Crinoids, intriguing marine animals within the Echinodermata phylum, have captured the interest of scientists for centuries. Historically significant to evolutionary biology, crinoids provide insights into the Cambrian explosion and subsequent echinoderm evolution [6]. Research on extant crinoids has been particularly robust from the early to mid-20th century, with more than 100 publications focusing on morphology, taxonomy, and classification [7,8]. The advent of molecular techniques has marked a new era in crinoid studies, with molecular phylogenetic methods shedding light on the evolutionary relationships among existing species [5,9–11]. Recent molecular studies, particularly concerning crinoid development, have underscored their unique life history and evolutionary trajectory [12–14]. For instance, Summers et al. conducted a molecular phylogenetic analysis on the Comatulidae family, reassessing morphological features for classification and proposing a new taxonomy [5,15]. This involved integrating molecular, morphological, behavioral, and biogeographic data to identify key traits and describe species. However, the current phylogeny of crinoids is undergoing significant revisions due to its instability [16]. Morphological traits are less reliable for classifying juvenile crinoids, which are smaller and more variable [17]. Robust molecular systematics are therefore critical for establishing consistent phylogenies.

Mitochondrial genomes have become invaluable in elucidating phylogenetic relationships and advancing evolutionary biology, thanks to features such as maternal inheritance and rapid evolutionary rates [18,19]. While mitochondrial research in crinoids has not been as extensive as in other groups, recent advancements in sequencing technology and enhanced sampling have started to bridge this gap. To date, complete mitochondrial genomes have been cataloged for two orders—Cyrtocrinida and Comatulida—and six families therein, including Sclerocrinidae, Colobometridae, Comatulidae [20], Antedonidae [21], Mariametridae [22] and Pentametrocrinidae [23].

To clearly understand crinoid phylogeny, this study presents the sequencing and annotation of mitochondrial genomes from 13 crinoid species spanning a range of depths and habitats. Our analysis aims to build upon the existing body of work by comparing new mitogenomic data with those from previous studies, which have typically been analyzed independently. Integrating new and existing datasets allows us to revisit and clarify the evolutionary history of crinoids. Our phylogenetic analysis supports the established idea that crinoids were ancestrally stalked, with stalkless forms evolving from these ancestors [11]. Interestingly, previous studies have shown that certain stalkless crinoids can secondarily become stalked.

By providing a detailed exploration of crinoid mitochondrial evolution, this study lays the groundwork for future research into the developmental and evolutionary aspects of crinoid biology.

## 2. Materials and Methods

### 2.1. Sample Collection and Mitogenome Sequencing

The samples were collected from various locations, including the Indian Ocean Ninety Degree Ridge, Carlsberg Ridge Seamount, Wuzhizhou Island, Sanya, Hainan, the East China Sea, Weizhou Island, Beihai, Guangxi, Hainan Xisha Ganquan Island, and the waters near Fuqing, Fujian, and Hainan Xisha Yongxing Island (Table 1). In this study, species within the order Comatulida have been classified as stalkless crinoids, whereas species belonging to the orders Hyocrinida, Isocrinida, and Cyrtocrinida are described as stalked crinoids.

**Table 1.** Species information, collection methods, and sampling locations.

Sampling Location	Collection Method	Species Name
Indian Ocean Ninety Degree Ridge	TV grab	<i>Thaumatocrinus</i> sp.
Carlsberg Ridge Seamount	TV grab	<i>Hyocrinidae</i> sp.
Wuzhizhou Island, Sanya, Hainan	Diving collection	<i>Comanthus parvicirrus</i>
Wuzhizhou Island, Sanya, Hainan	Diving collection	<i>Comanthus</i> sp.
Wuzhizhou Island, Sanya, Hainan	Diving collection	<i>Comaster schlegelii</i>
Wuzhizhou Island, Sanya, Hainan	Diving collection	<i>Comatella nigra</i>
East China Sea	Benthic trawl	<i>Capillaster</i> sp.
East China Sea	Benthic trawl	<i>Metacrinus rotundus</i>
East China Sea	Benthic trawl	<i>Ptilometra</i> sp.
Weizhou Island, Beihai, Guangxi	Diving collection	<i>Zygometa comata</i>
Hainan Xisha Ganquan Island	Diving collection	<i>Anneissia bennetti</i>
The waters near Fuqing, Fujian	Benthic trawl	<i>Tropiometra macrodiscus</i>
Hainan Xisha Yongxing Island	Diving collection	<i>Comatella stelligera</i>

After the surface mud stains were washed away, the samples were fixed with 100% ethanol and stored at  $-20\text{ }^{\circ}\text{C}$ . They were then transported to the laboratory for further processing. Crinoid barbs were separated and cleansed with sterilized distilled water. The total DNA was subsequently extracted using the EZNATM MicroElute Genomic DNA Kit (OMEGA, Buffalo, NY, USA), and its quality was verified by electrophoresis on a 1% agarose gel. Novogene Technology Co., Ltd. (Beijing, China) was engaged to construct a second-generation data database for the DNA that passed quality inspection. Using a Covaris ultrasonic breaker (Covaris, East Sussex, UK), the DNA was fragmented into pieces of 300–500 bp, which were then end-repaired by a double-strand enzyme. An ‘A’ base was added to the 3’ end of each fragment before attaching the double-strand sequencing adapters. This was followed by electrophoretic purification and bridge PCR amplification to finalize the next-generation sequencing library. Once the library passed quality control, it was calibrated according to effective concentration and the desired output volume for sequencing. Finally, sequencing was carried out using the Illumina Novaseq 2000 platform (PE150, 10×) in a paired-end configuration.

## 2.2. Mitogenome Assembly and Annotation

The raw sequence data were initially processed using Trimmomatic version 0.39 [24] (code: java -jar trimmomatic-0.39.jar PE -phred33 R1.fq R2.fq R1\_clean.fq R1\_un.fq R2\_clean.fq R2\_un.fq R2ILLUMINACLIP:TruSeq2-PE.fa:2:30:10:8:true LEADING:3 TRAILING:3 SLIDINGWINDOW:4:15 MINLEN:100) to trim adapters and low-quality sequences. Subsequent splicing and assembly were conducted using MitoZ version 3.0 [25]. The MITOS web service [26] was employed for the prediction of protein-coding genes (PCGs), transfer RNAs (tRNAs), and ribosomal RNAs (rRNAs). We performed a BLAST search [27] against the NCBI Nucleotide Collection (NR/NT) database based on the predicted mitochondrial gene. Alignment and subsequent correction of the protein-coding sequences were performed using MEGA X [28], followed by a comparison with previously published sequences of crinoid mitochondrial genomes. Complete assemblies of 13 mitochondrial genomes have been submitted to the GenBank database (see Table 2).

**Table 2.** Species information from mitochondrial phylogenetic analysis (the accession numbers of mitochondrial genomes provided in this study are in bold).

Order	Family	Species	Accession ID	Reference
Comatulida	Comatulidae	<i>Comaster schlegelii</i>	<b>MW526391</b>	this study
Comatulida	Comatulidae	<i>Comatella nigra</i>	<b>OM321037</b>	this study
Comatulida	Comatulidae	<i>Comanthus parvicirrus</i>	<b>MW526392</b>	this study
Comatulida	Comatulidae	<i>Comanthus</i> sp.	<b>OM272942</b>	this study
Comatulida	Charitometridae	<i>Capillaster</i> sp.	<b>OP546034</b>	this study

**Table 2.** Cont.

	Order	Family	Species	Accession ID	Reference
Ingroup	Comatulida	Ptilometridae	<i>Ptilometra</i> sp.	OP546035	this study
	Comatulida	Zygommetridae	<i>Zygommetra comata</i>	ON585667	this study
	Comatulida	Comatulidae	<i>Comatella stelligera</i>	OM313186	this study
	Comatulida	Comatulidae	<i>Anneissia bennetti</i>	ON209196	this study
	Comatulida	Tropiommetridae	<i>Tropiommetra macrodiscus</i>	ON381167	this study
	Comatulida	Pentametrocrinidae	<i>Thaumatoctrinus</i> sp.	OQ207656	this study
	Hyocrinida	Hyocrinidae	<i>Hyocrinidae</i> sp.	OQ721985	this study
	Isocrinida	Isselicrinidae	<i>Metacrinus rotundus</i>	OM964491	this study
	Cyrtocrinida	Sclerocrinidae	<i>Neogymnocrinus richeri</i>	DQ068951	[20]
	Comatulida	Antedonidae	<i>Poliometra proluxa</i>	OP177937	[29]
	Comatulida	Colobometridae	<i>Cenometra bella</i>	OK509084	[30]
	Comatulida	Comatulidae	<i>Anneissia intermedia</i>	MW376476	[31]
	Comatulida	Comatulidae	<i>Anneissia pinguis</i>	MW008594	[32]
	Comatulida	Antedonidae	<i>Antedon mediterranea</i>	NC_010692	NCBI
	Comatulida	Antedonidae	<i>Florometra serratissima</i>	AF049132	[21]
	Comatulida	Antedonidae	<i>Florometra</i> sp.	MT302206	[33]
	Comatulida	Pentametrocrinidae	<i>Thaumatoctrinus naresi</i>	OP428702	[23]
	Comatulida	Colobometridae	<i>Oligometra Serripinna</i>	MW405444	NCBI
	Comatulida	Comatulidae	<i>Phanogenia gracilis</i>	DQ068952	[20]
	Comatulida	Mariammetridae	<i>Stephanometra indica</i>	MF966246	[22]
Outgroup	Amphilepidida	Amphiuridae	<i>Amphipholis squamata</i>	FN562578	[34]
	Spatangoida	Loveniidae	<i>Echinocardium cordatum</i>	FN562581	[34]
	Valvatida	Solasteridae	<i>Crossaster papposus</i>	MW046047	[35]

### 2.3. Comparative Mitogenome Analyses

The crinoid mitochondrial genome sequence was analyzed using MEGA X [28] and PhyloSuite v.1.2.3 [36], including relative synonymous codon usage (RSCU), base composition, and amino acid composition. The relative usage of synonymous codons is calculated as  $RSCU = S \times Nc / Na$ , where ‘S’ represents the number of synonymous codons that encode the same amino acid, ‘Nc’ is the frequency of a particular codon within the genome, and ‘Na’ is the total count of all codons that encode that amino acid across the genome. This ‘Na’ serves as a measure of how frequently each synonymous codon is used relative to others that encode the same amino acid [37]. The calculation of the RSCU value reflects changes in coding efficiency and gene expression, which aids in understanding the evolution of the genetic code and the adaptive differences among populations [38]. The skewness of nucleotide composition was calculated using the following formulas:  $AT\text{-skew} = (A - T) / (A + T)$  and  $GC\text{-skew} = (G - C) / (G + C)$  [39]. To examine gene structure and variation across crinoid families, the 13 new mitochondrial genomes were compared to known crinoid sequences. Gene order rearrangements were analyzed using the online program CREx (<http://pacosy.informatik.uni-leipzig.de/crex>, accessed on 10 November 2023) [40].

### 2.4. Phylogenetic Analysis

Traditionally, echinoderm phylogeny has relied on morphology and fossils. Now, DNA and protein sequences are the main data for establishing phylogenies. Outgroups are added to determine the root. To study the phylogeny within the crinoid class, based on 13 PCGs and two ribosomal RNAs of 25 species of crinoids—using *A. squamata*, *E. cordatum*, and *C. papposus* as outgroups—the phylogenetic trees of crinoids were constructed using Bayesian inference (BI) and maximum likelihood (ML).

MAFFT v.7.505 software [41] was used for auto multiple-sequence alignment, and MACSE v.2 [42] was subsequently used to refine the alignment of the 15 genes. Gblocks v.0.91b software [43] was then utilized to eliminate inconsistent positions and divergent regions in the aligned sequences [44], making the final alignment more suitable for phylogenetic analysis. We utilized the concatenation function of PhyloSuite v.1.2.3 [36] to generate

concatenated files for the 15 genes. The optimal evolutionary model GTR + F + I + G4 was selected using ModelFinder (part of IQ-TREE v.1.6.8) [45]. Bayesian inference analysis using MrBayes 3.2 [46] was used for phylogenetic reconstruction with the following settings: 1,000,000 generations, four Markov-chain Monte Carlo chains, trees sampled every 100 generations, and an initial 25% of trees discarded as burn-in. Effective sample sizes (ESS) were monitored to ensure sufficient mixing and convergence of the MCMC chains. All parameter ESS values exceeded 200 after burn-in, indicating sufficient sampling. After the burn-in phase, we used the remaining trees to generate a 50% majority-rule consensus tree. Phylogenetic analyses were conducted with IQ-TREE v.1.6.8 [47], employing the maximum likelihood (ML) method with automatic model selection and 1000 ultrafast bootstrap replicates for tree support. Finally, the generated BI and ML phylogenetic trees were visualized using the iTOL (<http://itol.embl.de/>, accessed on 15 November 2023) [48].

### 2.5. Selection Pressure Analysis

Selection pressure analysis is a pivotal method for investigating how biological functional genes adapt to specific environmental conditions or factors. In our study, selection analyses were conducted using CODEML within the PAML 4.10 suite [49]. The nonsynonymous to synonymous substitution ratio (dN/dS) serves as a crucial metric for quantifying selective pressures acting on genetic sequences [50]. It is generally considered that synonymous mutations are not subject to natural selection, while nonsynonymous mutations are affected by natural selection. Typically, a dN/dS ratio greater than 1 indicates positive selection, suggesting that advantageous mutations are being selected for; a dN/dS ratio of 1 implies no selection, corresponding to neutral evolution; and a dN/dS ratio less than 1 but greater than 0 suggests purifying selection. The smaller the dN/dS value, the stronger the purifying selection pressure, indicating a more conserved amino acid sequence [51]. In these analyses, we designated stalked crinoids ( $n = 3$ ) as the foreground group and stalkless crinoids ( $n = 22$ ) as the background group. The rationale for selecting three stalked crinoids as the foreground clade for positive selection analysis is predicated on the unique genetic adaptations they may possess compared to their stalkless counterparts. Stalked crinoids, with their fixed lifestyle and close association with specific deep-sea substrates, may be subject to distinct metabolic and adaptive selection pressures on their mitochondrial genes.

We computed the dN/dS ratio for 13 mitochondrial protein-encoding genes, using a Bayesian phylogenetic tree of 25 crinoids as the guide. A single-proportion model was applied to estimate a uniform dN/dS ratio across all phylogenetic branches, and a branch-site model was employed to detect signatures of positive selection on the foreground branch specifically. The most suitable model within the nested set was determined using a likelihood ratio test (LRT), with the significance of the model appraised through a chi-square test ( $\chi^2$ ), comparing the  $2\Delta\ln L$  value against the chi-square distribution for the single-proportion model. Upon passing the LRT and exhibiting a statistically significant  $p$  value, the Bayesian Empirical Bayesian (BEB) approach [52] was utilized to identify sites of positive selection, denoting those with a posterior probability (PP) greater than 0.9 as candidates for positive selection. We identified amino acid sequences from positively selected sites. These sequences were used to model the three-dimensional structure of mitochondrial proteins. The proteins studied are the products of protein-coding genes (PCGs) from *M. rotundus*. For the modeling, we employed homology modeling techniques provided by the Swiss Model Server (<https://swissmodel.expasy.org>, accessed on 20 October 2023) [53–55].

## 3. Results

### 3.1. Mitogenome Structure and Organization

In this study, we expanded the crinoid mitogenome database by annotating 13 new species and analyzed the mitochondrial genomes of 25 species across 4 orders and 11 families. The lengths of the 25 complete mitochondrial genomes of crinoids range from 15,772 bp to 16,850 bp. All mitogenomes are circular and double-stranded molecular structures with

37 genes (22 tRNAs, 13 PCGs, 2 rRNAs). Among the 13 protein-coding genes, 10 are located on the heavy strand (H-strand), namely *cox1*, *cox2*, *cox3*, *atp6*, *atp8*, *nad3*, *nad4*, *nad4L*, *nad5*, and *cytb*, while the remaining genes are situated on the light strand (L-strand), including *nad1*, *nad2*, and *nad6*. Both ribosomal RNA genes (*rrnL* and *rrnS*) are found on the L-strand. All species showed a higher AT than GC content. The nucleotide composition of all protein-coding genes, as well as the rRNA genes, demonstrates a clear preference for A and T nucleotides.

The average contents of A, G, T, and C bases in these 25 mitogenomes were 25.08%, 16.82%, 46.48%, and 11.61%, respectively. The G base content of *N. richeri* and *Metacrinus rotundus* was higher than the A base content, while the remaining 23 species showed a higher A base content than the G base content. The A/T content ranged from 64.5% to 74.2% (Table S1), exhibiting an AT bias.

Among the 25 crinoids examined, including 13 that were newly sequenced, five distinct mitochondrial gene arrangement patterns have been identified (Figure 1). The predominant arrangement, found in 21 crinoid species, is categorized as pattern 1. In this pattern, the sequences of *rrnL* and *rrnS* genes are notably conserved, with *rrnL* located between *trnG* and *trnY*, and *rrnS* situated between *trnE* and *trnF*. Compared to pattern 1, the *trnI* gene in *Aneissia pinguis* (pattern 2) undergoes an inversion, shifting from the L-strand to the H-strand. Pattern 3 is represented by *Neogymnocrinus richeri*, where a translocation of the *nad4L* gene is observed. In *Tropiometra macrodiscus* (pattern 4), the gene clusters *trnR-nad4L* translocate from downstream of *cox1* gene to the upstream position of *trnS1* gene. Notably, the gene order of *Antedon mediterranea* (pattern 5) is basically consistent with that of *Tropiometra macrodiscus*, except for the translocation of *trnA* and *trnV* genes.

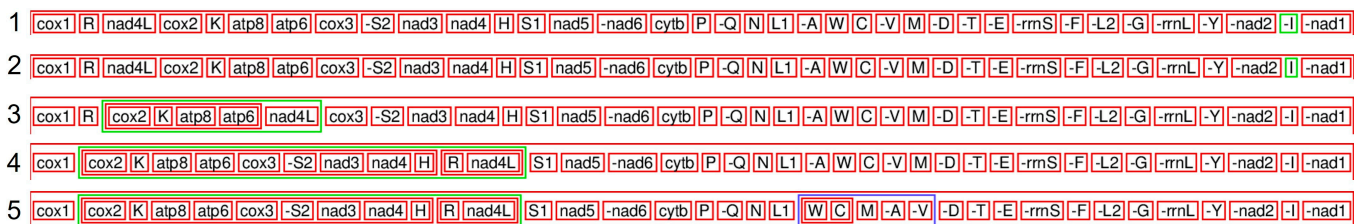


**Figure 1.** Five gene arrangement patterns of 25 crinoids (the symbol “—” denotes that the gene is located on the light strand (L-strand). In comparison to the gene order of pattern 1, sequence fragments that are rearranged in the other patterns are highlighted in green and blue marks. This figure was generated using the online program CREx.

### 3.2. Protein-Coding Genes

Among the 25 mitogenomes, 9 genes (*cox1-3*, *cytb*, *nad1-4*, and *nad6*) use “ATG” as the start codon, while the remaining 3 genes (*atp8*, *nad4L*, and *nad5*) have “GTG” codons (Table S2).

Eight PCGs (*atp6*, *atp8*, *cox2-3*, *nad3*, *nad4L* and *nad5-6*) terminate with complete stop codons (“TAA” or “TAG”), while five genes (*cox1*, *cytb*, *nad1-2*, and *nad4*) have incomplete stop codons (“TA-” or “T-”) in some crinoids. More specifically, the *cox1* and *cytb* genes use “TA”, while *cytb*, *nad1*, *nad2*, and *nad4* have terminal “T” (Table S3).

RSCU analysis indicates a marked preference for specific codons, including UCU, UUA, GUU, CCU, and GCU, across the protein-coding genes (PCGs) of 25 crinoid mitogenomes (Figure 2). Notably, the UCU codon is highly favored in *Hyocrinidae* sp., and UUA is favored in *Comatella stelligera*, both exhibiting significant overexpression with an RSCU value of 3.94, suggesting a strong codon bias. In contrast, the UUA codon, which codes for leucine (Leu2), is underrepresented in *Neogymnocrinus richeri* and *Metacrinus rotundus* when compared to other crinoids, indicating a unique codon usage pattern in these species that could be reflective of evolutionary or adaptive differences.

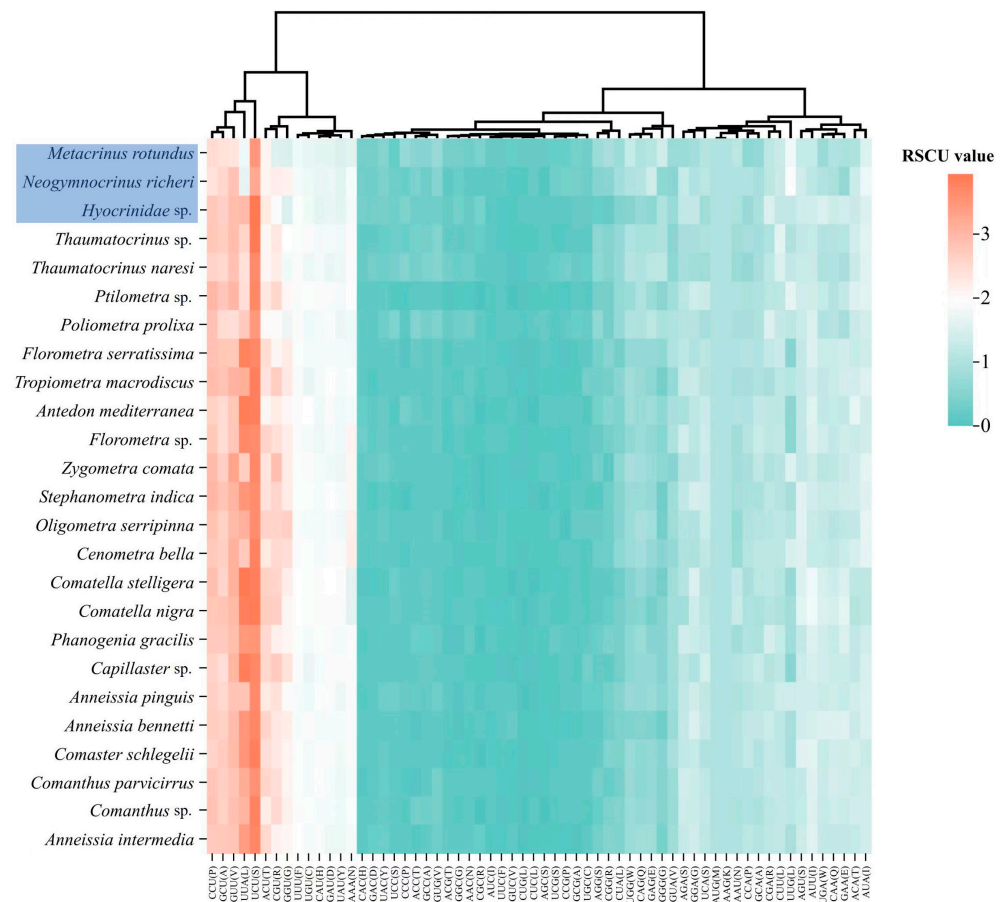


**Figure 2.** Relative synonymous codon usage (RSCU) and codon distribution in PCGs of 25 crinoid mitogenomes (the symbols in brackets on the X-axis represent the amino acid corresponding to each codon and use the one-letter nomenclature for that amino acid). Stalked crinoids in the Y-axis are highlighted with a blue background. Orange: high RSCU value; green: low RSCU value. This figure was generated using Origin 2018 [56].

### 3.3. Phylogenetic Analyses

Phylogenies were constructed using 13 PCGs and 2 rRNAs from 25 crinoid taxa and outgroups, with Bayesian inference (BI) and maximum likelihood (ML) approaches (Figures 3 and 4). Except for the outgroup and the Ptilometridae family, the phylogenetic trees generated by the two approaches are nearly identical at the family and order levels of topology. The phylogenetic relationship among the four orders is (Isocrinida + (Cyrtoctrinida + (Hyocrinida + Comatulida))). As shown in Figure 4, the order Comatulida has three main phylogenetic clades: (1) Pentametrocrinidae, (2) Comatulidae, and (3) a clade represented by the remaining families, including Ptilometridae, Tropiometridae, Antedonidae, Himerometridae, Stephanometridae, and Colobometridae.

More specifically, *Thaumatoctrinus* sp. and *Thaumatoctrinus naresi* are separately aggregated into the first clade of the Comatulida order (Figures 3 and 4). In the second clade, the Comatulidae family is divided into two branches, namely the Comatellinae subfamily (*Comatella nigra* and *Comatella stelligera*) and the Comatulinae subfamily (the other five genera). Furthermore, the *Anneissia* genus seems to be a polyphyletic lineage due to the separation of its species into *Anneissia intermedia*.

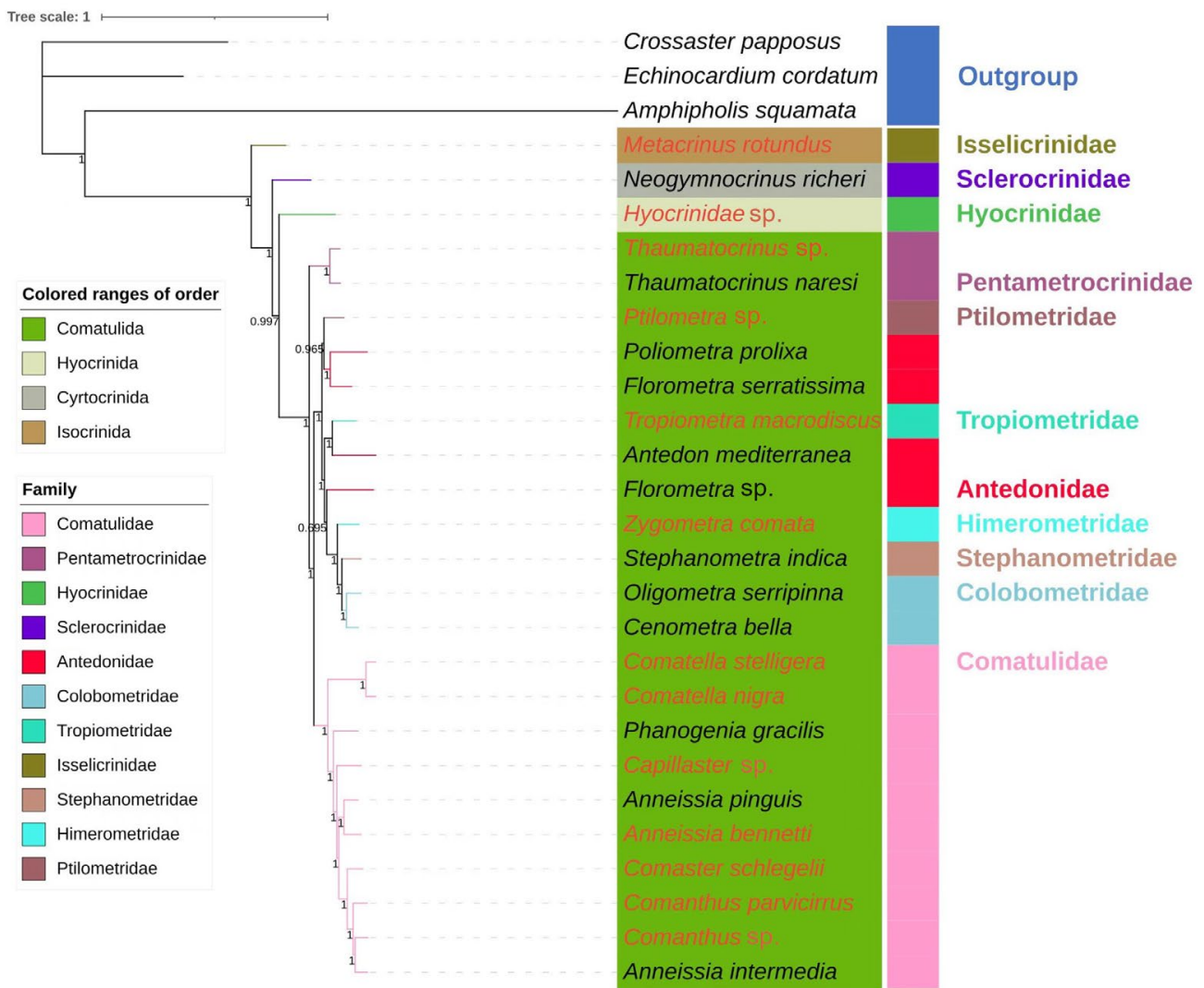


**Figure 3.** Bayesian phylogenetic tree constructed based on 13 PCGs and 2 rRNA genes (the species marked in red are the species sequenced in this study; posterior probabilities values are indicated above nodes). This figure was generated using iTOL (<http://itol.embl.de/>, accessed on 15 November 2023).

For the third phylogenetic clade within the Comatulida order, the Himerometridae, Stephanometridae, and Colobometridae families are supported as a monophyletic sister group, receiving strong bootstrap support in the ML analysis and high posterior probabilities in the BI analysis. Moreover, the evolutionary relationship of the Ptilometridae family within this third clade is ambiguous, and we need more molecular data to illuminate this.

Notably, the Antedonidae family is polyphyletic, with its species divided into three main branches based on the BI analysis. For instance, *Antedon mediterranea* and *Tropiometra macrodiscus* are depicted as an isolated lineage, reflecting their independent evolutionary histories. For the *Florometra* genus, two species fail to cluster together, but instead separately group with other genera. These results hint that feather stars have a complex evolutionary relationship that may warrant further investigation to elucidate.



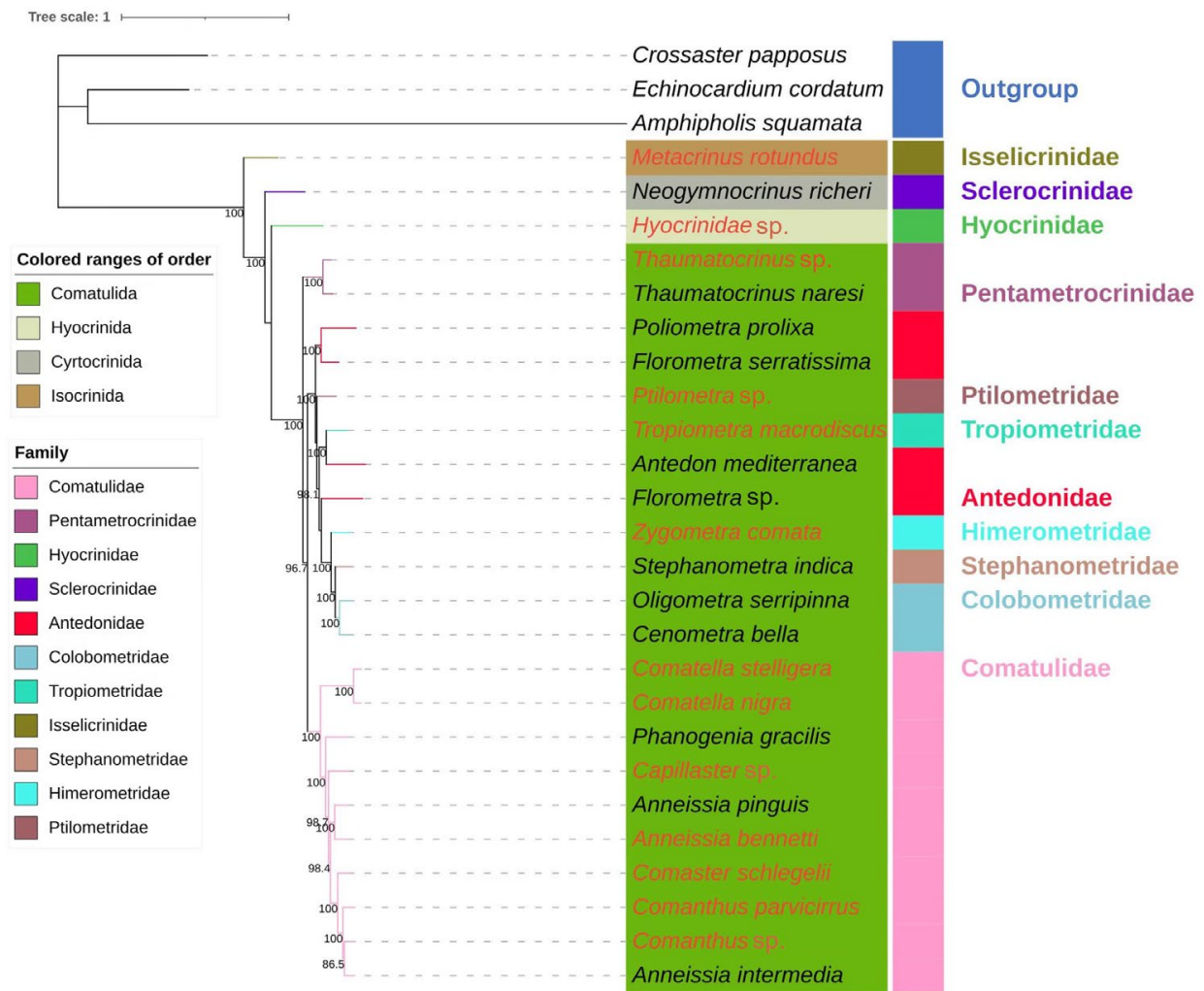


**Figure 4.** Maximum likelihood phylogenetic tree constructed based on 13 PCGs and 2 rRNA genes (the species marked in red are the species sequenced in this study; bootstrap support values were indicated above nodes). This figure was generated using iTOL (<http://itol.embl.de/>, accessed on 15 November 2023).

### 3.4. Relaxed Selective Constraint and Positive Selection on the Mitochondrial Genes

Incorporating the three stalked crinoids as the foreground clade, the results of the single-ratio model showed that all PCGs exhibited a dN/dS ratio <1 (Table S4 and Figure 5), indicating purifying selection. Most PCGs have similar dN/dS ratios in both types of crinoids, suggesting comparable evolutionary pressures. Particularly noteworthy are the dN/dS ratios for *atp8* in the foreground group, which decreased significantly to 0.0013 from 0.1256 in the background, suggesting an intensified purifying selection in the stalked crinoids.

In contrast, *nad2* exhibited a slight increase in its dN/dS ratio from 0.06 in the background group to 0.0722 in the foreground, suggesting a relaxation in purifying selection, though the value still denotes purifying selection overall. This subtle change hints at potential variations in metabolic demands or mitochondrial function between the two groups. Other genes such as *nad3*, *nad4*, and *nad5*, while also under purifying selection, showed smaller differences in their dN/dS ratios between the foreground and background groups, which does not suggest positive selection but rather minor variations in the strength of purifying selection.

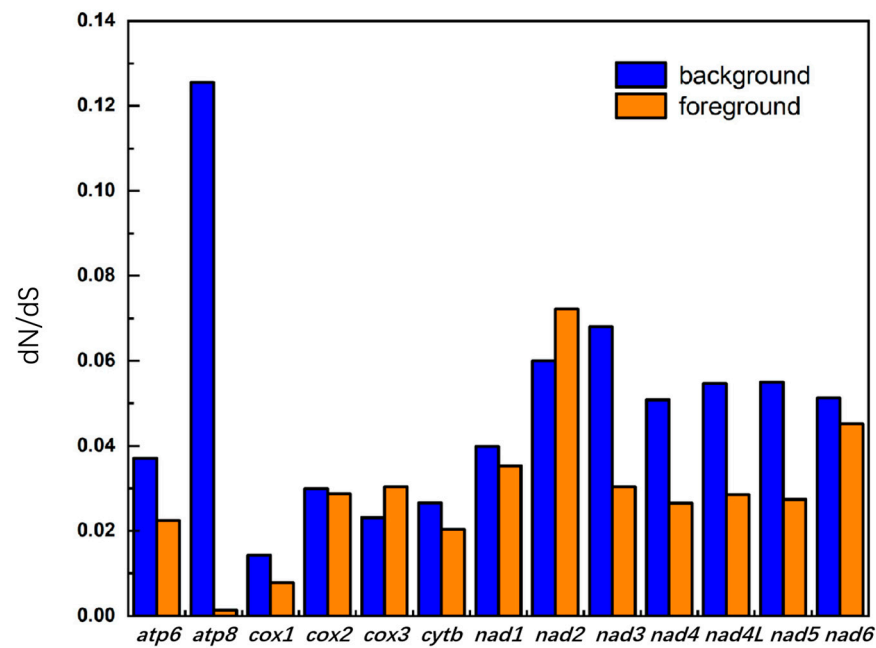


**Figure 5.** The ratio of nonsynonymous to synonymous substitutions (dN/dS) for 13 PCGs in 25 crinoids (with stalked crinoids as the foreground group and stalkless crinoids as the background group), generated using Origin 2018 [56].

The existing literature and preliminary studies suggest that these adaptive changes could play a pivotal role in the evolutionary trajectory of their mitochondrial genes [57]. Consequently, we focused on identifying signals of adaptive positive selection within this group’s mitochondrial genes. Notably, when the analysis was conducted with 22 stalkless crinoids as the foreground clade, no positive selection sites were detected, further substantiating our hypothesis that stalked crinoids may have undergone specific adaptive evolutionary processes.

Branch-site model analysis revealed eleven positively selected sites across six mitochondrial PCGs in stalked crinoids (Table 3). Four of these sites showed Bayes Empirical Bayes posterior probability over 0.99, indicating very strong positive selection signals. These included serine at site 2020 of *nad2*; serine at site 2344 of *nad3*; lysine at site 2568 of *nad4*; and serine at site 3244 of *nad5*. The remaining seven sites also showed high posterior probabilities between 0.954 and 0.987. The high probabilities of positive selection suggest these amino acid replacements likely conferred selective advantages during the evolution of stalked crinoids.

**Table 3.** Positively selected sites and genes in lineages under positive selection as indicated by Bayesian Empirical Bayesian (BEB) analysis. \* BEB posterior probability > 95%; \*\* BEB posterior probability > 99%.

Gene	Site
<i>cytb</i>	1492 I 0.955 *
	2020 S 0.996 **
<i>nad2</i>	2044 R 0.954 *
	2174 C 0.977 *
	2344 S 0.995 **
<i>nad3</i>	2344 S 0.995 **
<i>nad4L</i>	2495 F 0.977 *
<i>nad4</i>	2568 K 0.999 **
	2691 S 0.987 *
<i>nad5</i>	3124 N 0.967 *
	3244 S 0.994 **
	3403 K 0.954 *

To comprehensively assess the effects of positive selection sites and the alterations in physicochemical properties resulting from amino acid substitutions, we mapped the positive selection sites, identified by CODEML in *M. rotundus* species, onto the corresponding mitochondrial protein structure. Remarkably, our findings revealed that a significant proportion of the identified positively selected sites were situated within or near functional regions (Figure 6). This emphasizes their potential role in evolutionary adaptation.

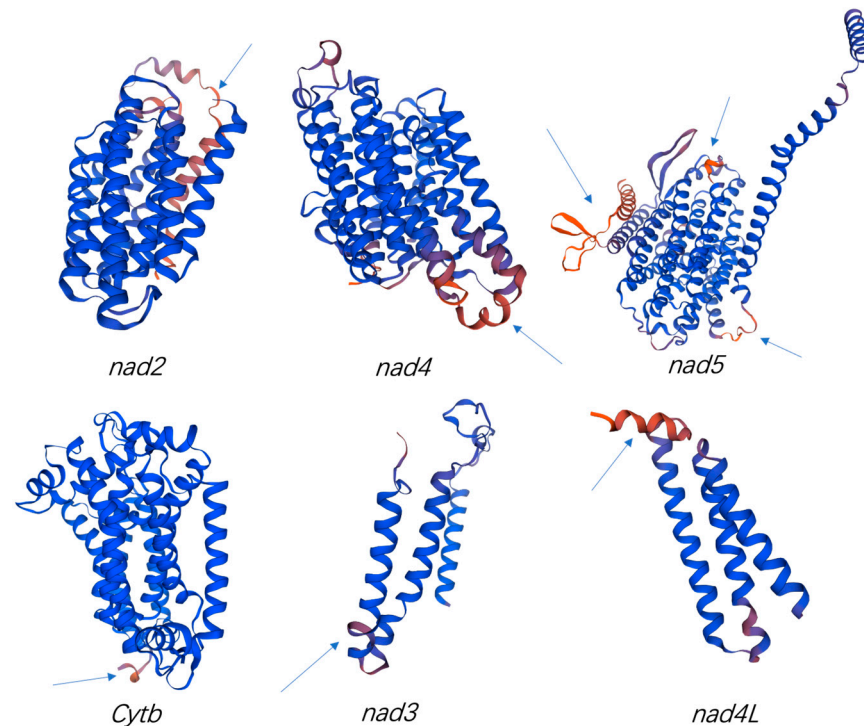


**Figure 6.** Atomic-level structures of computationally predicted mitochondrial protein-coding genes (*nad2–nad5*, *nad4L*, and *cytb*) of *M. rotundus*. Positively selected sites inferred by CODEML are shown in red; all sites identified by these methods are shown in orange and highlighted with arrows.

## 4. Discussion

### 4.1. Mitochondrial Genome Structural Characteristics

In our phylogenetic analysis, *N. richeri* and *M. rotundus* emerge as basal taxa, providing a unique vantage point to explore the ancestral states of nucleotide composition. Notably, we observed a pronounced evolutionary shift from guanine (G) to adenine (A) bases within these lineages, indicative of an overarching trend towards an AT bias. This bias is not merely a relic of past mutational events but appears to be a dynamic feature sustained over evolutionary timescales.

Mitochondrial DNA (mtDNA) tends to mutate faster than nuclear DNA, often resulting in a higher occurrence of adenine (A) and thymine (T) bases, which contributes to a condition known as AT bias. The tendency for AT enrichment may partly derive from the susceptibility of mtDNA to oxidative damage coupled with distinctive aspects of its replication process. Sequences with a higher AT content tend to be less stable compared to those rich in guanine (G) and cytosine (C), predisposing them to a more frequent mutational occurrence. Consequently, this can substantially alter the base composition of mtDNA. While this shift may be attributable in part to the known vulnerability of the light strand to mutation during replication, leading to the observed base composition [39], it is plausible that selective pressures have also played a role [58]. Moreover, this finding aligns with previous studies that have reported a similar AT bias in crinoid mitochondrial genomes [20,21], suggesting that the light strand's proclivity for higher mutation rates could be a widespread phenomenon [59].

Echinoderm mitogenomes typically utilize an “ATG” start codon [60] and incomplete stop codons [61]. This study showed that not only *nad4L* and *nad5* [20,21] but also *atp8* initiated with “GTG”. In other echinoderms, *atp8* was also found to have “GTG” as the initiation codon [62–64]. Of the 13 sequenced mitogenomes in this study, all PCGs except *cytb* terminated with complete stops (“TAA” or “TAG”). *Cytb* in six species (*Comanthus parvicirrus*, *Comanthus* sp., *T. macrodiscus*, *Capillaster* sp., *Anneissi. bennetti*, and *Hyocrinidae* sp.) used an incomplete “T” stop codon.

The balance between base mutation bias and natural selection is expressed as codon bias [65,66]. In 23 crinoid species except *N. richeri* and *M. rotundus*, the content of the A base was higher than that of the G base. In *N. richeri* and *M. rotundus*, the UUA codon for leucine Leu2 is under-expressed relative to other stalked crinoids. We hypothesize that the imbalance in nucleotide composition, specifically the asymmetry between the strands in mitochondrial DNA, contributes to the observed preferences in codon usage among these crinoid species.

Here, we expand upon the significance of asymmetric PCG codon usage. The asymmetric usage of codons, where H-strand genes prefer G/T terminal codons and L-strand genes favor A/C terminal codons [67], may have substantial implications for mitochondrial genome function and evolution in crinoids. Such biases in codon usage can influence gene expression levels, potentially due to the differential availability of tRNA and the efficiency of the translation process [68]. Additionally, these biases could impact the speed and accuracy of protein synthesis, affecting protein folding and function [69]. In the context of mitochondrial genomes, these codon biases may reflect the organism’s adaptations to specific energetic and metabolic demands [38]. The under-expression of the UUA codon for leucine (Leu2) in *N. richeri* and *M. rotundus* may indicate the adaptation of their mitochondrial genomes to their unique ecological niches, characterized by factors such as temperature, salinity, and available energy resources. These environmental factors could exert selective pressures that favor certain mitochondrial codon usages over others, leading to more efficient protein synthesis in the specific habitats in which these crinoids thrive.

In our study, 25 species of crinoid mitogenomes exhibited five arrangement patterns. Mitogenome arrangement can reveal the phylogenetic relationship between different species [70,71]. In recent years, several studies on the arrangement of mitochondrial genes in echinoderms have been reported [62,72]. Crinoidea [62] and Ophiuroidea [73,74] exhibit greater gene order variability than other echinoderms. The mitogenome order varies most in Crinoidea; some crinoids (e.g., *A. mediterranea* and *N. richeri*) no longer showed conserved gene blocks present in the other four echinoderm classes [75].

#### 4.2. Phylogenetic Relationships

At present, echinoderm phylogenetics traditionally focuses on interphyla and interclass relationships. Crinoids occupy a pivotal position in the phylogenetic tree of echinoderms [34], yet their intraclass evolutionary relationships, especially through the lens of mitochondrial genomes, remain underexplored. Our study aims to fill this gap by utilizing mitochondrial genome sequences to construct phylogenetic trees, thus providing a new insight into the intraclass relationships among crinoids using this molecular approach. In this study, we used *A. squamata*, *E. cordatum*, and *C. papposus* as outgroups, and constructed Bayesian and ML phylogenetic trees with 25 species.

Inferred phylogenetic relationships from the ML analysis, based on the concatenated fifteen-gene complete dataset (PCGs and rRNA genes of mitochondrial genomes) within the Himerometroididea [76], corroborate previous findings suggesting a close kinship among Himerometridae, Stephanometridae, and Colobometridae. The phylogenetic relationships within the Antedonidae family are complex. Currently, related studies based on molecular data (*COI*, *16S*, *28S*, and *ITS*), morphology, and multivariate analyses show that the Antedonidae family is a polyphyletic group [11]. Our study also extends this insight by demonstrating that two species from the Antedonidae and Tropiometridae families exhibit a close genetic relationship, clustering as an isolated lineage. In addition, they both exist as

translocations of *nad4L* and *trnR*, suggesting that these translocations may be conserved in this lineage. Moreover, two species of the *Florometra* genus within the Antedonidae family separately group with other genera. Meanwhile, this same inconsistency is obvious for *Anneissia* species from the Comatulidae family. This genetic closeness and inconsistency, however, present a conundrum regarding the taxonomic delineations within Antedonidae and Comatulidae, as our data suggest a potential revision of their classification may be necessary.

The widespread distribution and diverse habitats of the Crinoidea class have given rise to an extensive variety of morphological features, demonstrating notable variation even among species that are closely related. This morphological plasticity often complicates species' identification and may lead to misclassifications. The current findings emphasize the utility of molecular data in providing clarity and resolving ambiguities that morphological analyses alone may not adequately address [77]. Such discrepancies highlight the need for a taxonomic reassessment that incorporates both molecular and morphological data to ensure accurate species classification and a deeper understanding of crinoid diversity [78,79].

#### 4.3. Positive Selection Site

Natural selection is widely recognized as a key evolutionary force [80]. Mitochondrial genes are considered to undergo purifying selection to maintain function [81]. Positively selected genes drive adaptive evolution [82]. The dN/dS ratio indicates the evolutionary rate [83–86]. There remains a significant debate concerning whether positive selection or purifying selection prevails.

All 13 PCGs exhibited a dN/dS ratio < 1, signifying prevalent negative selection that acts to remove deleterious mutations while preserving conserved amino acid sequences. This observation is consistent with the known functions of mitochondrial genes, as changes in these genes can significantly impact an organism's survival. Notably, the dN/dS ratio for *atp8* was significantly higher in stalkless crinoids (0.1256) compared to stalked crinoids (0.0013). This difference may suggest that stalkless crinoids either face reduced selective constraints or have advantageous mutations in the *atp8* gene that confer adaptive benefits. Such advantageous mutations in the *atp8* gene could have significant implications for the evolution of the mitochondrial genome. They might lead to compensatory evolutionary changes in other mitochondrial genes, a phenomenon we refer to as 'compensatory draft feedback', where alterations in one part of the genome necessitate or drive changes in another to maintain overall mitochondrial function and efficiency [87,88]. Species under significant negative selection may evolve faster to maintain mitochondrial function. Therefore, the *atp8* gene may play a crucial role in the mitogenomic evolution of stalkless crinoids. Compared to stalkless crinoids, stalked crinoids showed lower dN/dS ratios for *nad3*, *nad4*, and *nad5*, suggesting stronger negative selection on more essential functions. The ineffectiveness of negative selection allows for the accumulation of deleterious mutations [89].

Divergent PCG selection sites between crinoid groups distributed across *cytb*, *nad2*, *nad3*, *nad4L*, *nad4*, and *nad5* indicate adaptive diversification. Positively selected sites within the *cytb* gene, particularly in regions critical to its function, suggest that deep-sea crinoids may have evolved adaptations to their extreme habitats. These modifications could enhance the efficiency of oxidative phosphorylation [90], allowing these organisms to optimize energy production in low-oxygen environments. *Nad* genes encode electron transport proteins [91], with *nad2*, *nad4*, and *nad5* integral to proton pumping [92]. Furthermore, changes in the *Nad* genes, which encode components of the electron transport chain, may result in proteins that are better suited to the unique features of deep-sea life [93] such as high pressure and cold temperatures. Such adaptations could lead to increased metabolic efficiency, allowing these crinoids to survive and function effectively where resources are scarce and conditions are challenging. The deep sea features anoxia, darkness, high pressure, and low temperatures [94]. Under these extreme environmental conditions,

organisms may require improved and adapted energy metabolism. Positive selection sites in *nad* family genes, found in a variety of deep-sea species such as corals [95], sea cucumber [96], mussels [97], and starfish [98], suggest specific evolutionary adjustments. These sites may alter the structure and function of the NADH dehydrogenase complex, which could lead to variations in the efficiency of the electron transport chain. For example, modifications in the gene products might improve the organism's ability to generate energy under the low-oxygen conditions of the deep sea. Enhanced energy production could, in turn, influence the organism's resilience to the high pressures and cold temperatures characteristic of these environments.

## 5. Conclusions

This study markedly extends the crinoid mitochondrial genome database by adding 13 newly sequenced genomes, thus providing new resources for future research. Such expansions in the database not only facilitate the identification of species-specific mitochondrial markers but also underpin the comparative studies necessary for resolving the complex phylogenetic relationships within the Echinodermata. The identification of five mitochondrial gene arrangement patterns offers profound insights into the evolutionary processes of crinoids. These patterns represent genomic structural variations that may correlate with key ecological and evolutionary transitions in crinoid history, such as changes in habitat or feeding strategies. By examining the variations in gene arrangements alongside the phylogenetic information, we can begin to unravel the adaptive significance behind these mitochondrial configurations. Arrangement comparisons of the mitochondrial genome may be useful for phylogenetic reconstruction. Moreover, additional molecular data are essential to deepen our understanding of how mitochondrial gene arrangement contributes to the evolution of crinoids.

Our selective pressure analysis revealed positive selection in several genes—*cytb*, *nad2*, *nad3*, *nad4*, *nad4L*, and *nad5*—indicating adaptive evolution at the molecular level. These genes, integral to the respiratory chain, may have evolved under selective pressures to optimize energy production, which is critical for crinoid survival in diverse marine environments.

The monophyly of crinoid families remains a topic of debate, with in-depth phylogenetic studies being scarce. Based on the mitochondrial genome data, our phylogenetic reconstruction reveals the polyphyly of certain genera and families within the Comatulida order. This result not only offers molecular insights into crinoid phylogenetic relationships but also uncovers the intricate tapestry of their evolutionary history. Providing a statistical backbone to these findings, such as bootstrap values and posterior probabilities, strengthens our confidence in these phylogenetic interpretations and invites further investigation into the evolutionary mechanisms at play. As we amass new mitochondrial genome data, it is equally important to collect more nuclear data, such as *ITS*, *18S rRNA*, *28S rRNA*, and *Histone H3*. Combining both mitochondrial and nuclear sequence data is likely to yield more comprehensive and accurate results.

Furthermore, our study sheds light on the potential of mitochondrial markers in species identification and phylogenetics in crinoids, asserting their utility in this domain. Practical applications of these enhanced mitochondrial markers may include the development of more precise conservation strategies or the implementation of mitogenomic tools in monitoring biodiversity and ecosystem health.

**Supplementary Materials:** The following supporting information can be downloaded at: <https://www.mdpi.com/article/10.3390/jmse12030361/s1>, Table S1: Base composition of mitochondrial genomes of 25 crinoids; Table S2: Putative start codon of 13 PCGs in 25 crinoids; Table S3: Putative terminal codon of 13 PCGs in 25 crinoids; Table S4. The ratio of nonsynonymous to synonymous substitutions (dN/dS) for 13 PCGs in 25 crinoids with stalked crinoids as the foreground group and stalkless crinoids as the background group.

**Author Contributions:** Conceptualization, Q.X. and X.H. (Xuebao He); Funding acquisition, Q.X.; Investigation, Z.L.; Project administration, Q.X.; Validation, Y.L.; Visualization, Y.D.; Writing—original draft, Q.X., M.L. and Y.S.; Writing—review and editing, X.H. (Xuying Hu), Q.Z. and B.L. All authors have read and agreed to the published version of the manuscript.

**Funding:** This research was funded by the National Natural Science Foundation of China (42176135).

**Institutional Review Board Statement:** Not applicable.

**Informed Consent Statement:** Not applicable.

**Data Availability Statement:** The mitogenomes were deposited at NCBI, with accession numbers MW526391, OM321037, MW526392, OM272942, OP546034, OP546035, ON585667, OM313186, ON209196, ON381167, OQ207656, OQ721985, and OM964491.

**Conflicts of Interest:** The authors declare no conflicts of interest.

## References

1. Ausich, W.I.; Brett, C.E.; Hess, H.; Simms, M.J. Crinoid form and function. In *Fossil Crinoids*; Cambridge University Press: Cambridge, UK, 1999; Volume 1, pp. 3–30.
2. Wada, H.; Satoh, N. Phylogenetic relationships among extant classes of echinoderms, as inferred from sequences of 18S rDNA, coincide with relationships deduced from the fossil record. *J. Mol. Evol.* **1994**, *38*, 41–43. [[CrossRef](#)] [[PubMed](#)]
3. Roux, M.; Messing, C.G.; Améziane, N. Artificial keys to the genera of living stalked crinoids (Echinodermata). *Bull. Mar. Sci.* **2002**, *70*, 799–830.
4. Messing, C.G. Living comatulids. *Paleontol. Soc. Pap.* **1997**, *3*, 3–30. [[CrossRef](#)]
5. Summers, M.M.; Messing, C.G.; Rouse, G.W. The genera and species of Comatulidae (Comatulida: Crinoidea): Taxonomic revisions and a molecular and morphological guide. *Zootaxa* **2017**, *4268*, 151–190. [[CrossRef](#)] [[PubMed](#)]
6. Rozhnov, S. The onset of the Ordovician evolutionary radiation of benthic animals in the Baltic Region: Explosive diversity of attachment structures of stalked echinoderms, substrate revolution and the role of cyanobacterial communities. *Palaeoworld* **2019**, *28*, 110–122. [[CrossRef](#)]
7. Clark, A.H. *A monograph of the existing crinoids*; US Government Printing Office: Washington, DC, USA, 1967.
8. Clark, A. Monograph of existing crinoids, part 2: Parasites and commensals. *United States Natl. Mus. Bull.* **1921**, *82*, 616–660.
9. Cohen, B.L.; Améziane, N.; Eleaume, M.; de Forges, B.R. Crinoid phylogeny: A preliminary analysis (Echinodermata: Crinoidea). *Mar. Biol.* **2004**, *144*, 605–617. [[CrossRef](#)]
10. Hemery, L.G.; Roux, M.; Améziane, N.; Eleaume, M. High-resolution crinoid phyletic inter-relationships derived from molecular data. *Cah. De Biol. Mar.* **2013**, *54*, 511–523.
11. Rouse, G.W.; Jermin, L.S.; Wilson, N.G.; Eeckhaut, I.; Lanterbecq, D.; Oji, T.; Young, C.M.; Browning, T.; Cisternas, P.; Helgen, L.E. Fixed, free, and fixed: The fickle phylogeny of extant Crinoidea (Echinodermata) and their Permian–Triassic origin. *Mol. Phylogenetics Evol.* **2013**, *66*, 161–181. [[CrossRef](#)]
12. Nakano, H.; Nakajima, Y.; Amemiya, S. Nervous system development of two crinoid species, the sea lily *Metacrinus rotundus* and the feather star *Oxycomanthus japonicus*. *Dev. Genes Evol.* **2009**, *219*, 565–576. [[CrossRef](#)]
13. Mercurio, S.; Gattoni, G.; Messinetti, S.; Sugni, M.; Pennati, R. Nervous system characterization during the development of a basal echinoderm, the feather star *Antedon mediterranea*. *J. Comp. Neurol.* **2019**, *527*, 1127–1139. [[CrossRef](#)] [[PubMed](#)]
14. Omori, A.; Shibata, T.F.; Akasaka, K. Gene expression analysis of three homeobox genes throughout early and late development of a feather star *Anneissia japonica*. *Dev. Genes Evol.* **2020**, *230*, 305–314. [[CrossRef](#)]
15. Summers, M.M.; Messing, C.G.; Rouse, G.W. Phylogeny of Comatulidae (Echinodermata: Crinoidea: Comatulida): A new classification and an assessment of morphological characters for crinoid taxonomy. *Mol. Phylogenetics Evol.* **2014**, *80*, 319–339. [[CrossRef](#)]
16. Wright, D.F.; Ausich, W.I.; Cole, S.R.; Peter, M.E.; Rhenberg, E.C. Phylogenetic taxonomy and classification of the Crinoidea (Echinodermata). *J. Paleontol.* **2017**, *91*, 829–846. [[CrossRef](#)]
17. Huang, D. Phylogeny and morphology of Himerometroidea (Echinodermata: Crinoidea) feather stars in Singapore. *Raffles Bull. Zool.* **2023**, *71*, 92–105.
18. Curole, J.P.; Kocher, T.D. Mitogenomics: Digging deeper with complete mitochondrial genomes. *Trends Ecol. Evol.* **1999**, *14*, 394–398. [[CrossRef](#)]
19. Priyono, D.S.; Solihin, D.D.; Farajallah, A.; Purwantara, B. The first complete mitochondrial genome sequence of the endangered mountain anoa (*Bubalus quarlesi*) (Artiodactyla: Bovidae) and phylogenetic analysis. *J. Asia-Pac. Biodivers.* **2020**, *13*, 123–133. [[CrossRef](#)]
20. Scouras, A.; Smith, M.J. The complete mitochondrial genomes of the sea lily *Gymnocrinus richeri* and the feather star *Phanogenia gracilis*: Signature nucleotide bias and unique nad4L gene rearrangement within crinoids. *Mol. Phylogenetics Evol.* **2006**, *39*, 323–334. [[CrossRef](#)] [[PubMed](#)]

21. Scouras, A.; Smith, M.J. A novel mitochondrial gene order in the crinoid echinoderm *Florometra serratissima*. *Mol. Biol. Evol.* **2001**, *18*, 61–73. [[CrossRef](#)] [[PubMed](#)]
22. Ma, S.; Zhang, H.; Wang, X.; Yin, J.; Shen, P.; Lin, Q. Characterization and phylogenetic analysis of the complete mitochondrial genome of *Stephnometra indica* (Pelmatozoa: Crinoidea). *Mitochondrial DNA Part B* **2019**, *4*, 2283–2284. [[CrossRef](#)]
23. Lin, Q.; Zhang, R.; Wang, C. The mitochondrial genome of a 9-arm feather star *Thaumatocrinus naresi* (Crinoidea, Pentametocrinidae). *Mitochondrial DNA Part B* **2023**, *8*, 368–370. [[CrossRef](#)]
24. Bolger, A.M.; Lohse, M.; Usadel, B. Trimmomatic: A flexible trimmer for Illumina sequence data. *Bioinformatics* **2014**, *30*, 2114–2120. [[CrossRef](#)]
25. Meng, G.; Li, Y.; Yang, C.; Liu, S. MitoZ: A toolkit for animal mitochondrial genome assembly, annotation and visualization. *Nucleic Acids Res.* **2019**, *47*, e63. [[CrossRef](#)] [[PubMed](#)]
26. Bernt, M.; Donath, A.; Jühling, F.; Externbrink, F.; Florentz, C.; Fritzsche, G.; Pütz, J.; Middendorf, M.; Stadler, P.F. Mitos: Improved de novo metazoan mitochondrial genome annotation. *Mol. Phylogenetics Evol.* **2013**, *69*, 313–319. [[CrossRef](#)] [[PubMed](#)]
27. Johnson, M.; Zaretskaya, I.; Raytselis, Y.; Merezukh, Y.; McGinnis, S.; Madden, T.L. NCBI BLAST: A better web interface. *Nucleic Acids Res.* **2008**, *36*, W5–W9. [[CrossRef](#)]
28. Kumar, S.; Stecher, G.; Li, M.; Nnyaz, C.; Tamura, K. MEGA X: Molecular evolutionary genetics analysis across computing platforms. *Mol. Biol. Evol.* **2018**, *35*, 1547. [[CrossRef](#)]
29. Kwon, H.; Park, H.S.; Rhee, J.-S. Complete mitochondrial genome of the crinoid *Poliometra proluxa* (Crinoidea: Comatulida: Antedonidae). *Mitochondrial DNA Part B* **2023**, *8*, 927–931. [[CrossRef](#)] [[PubMed](#)]
30. Chang, J.J.M.; Ip, Y.C.A.; Huang, D. Complete mitochondrial genome of the feather star *Cenometra bella* (Hartlaub, 1890)(Crinoidea: Colobometridae). *Mitochondrial DNA Part B* **2022**, *7*, 950–952. [[CrossRef](#)]
31. Kim, P.; Lee, T.; Shin, S. The complete mitochondrial genome of *Anneissia intermedia* (Crinoidea: Comatulida: Comatulidae). *Mitochondrial DNA Part B* **2021**, *6*, 1777–1778. [[CrossRef](#)]
32. Kim, P.; Shin, S. The complete mitochondrial genome of *Anneissia pinguis* (Crinoidea, Articulata, Comatulidae), from South Korea. *Mitochondrial DNA Part B* **2021**, *6*, 2337–2338. [[CrossRef](#)]
33. Nam, S.-E.; Park, H.S.; Rhee, J.-S. Characterization and phylogenetic analysis of the complete mitochondrial genome of *Florometra* species (Echinodermata, Crinoidea). *Mitochondrial DNA Part B* **2020**, *5*, 2010–2011. [[CrossRef](#)]
34. Perseke, M.; Bernhard, D.; Fritzsche, G.; Brümmer, F.; Stadler, P.F.; Schlegel, M. Mitochondrial genome evolution in Ophiuroidea, Echinoidea, and Holothuroidea: Insights in phylogenetic relationships of Echinodermata. *Mol. Phylogenetics Evol.* **2010**, *56*, 201–211. [[CrossRef](#)] [[PubMed](#)]
35. Nam, S.-E.; Kim, S.A.; Park, T.-Y.S.; Rhee, J.-S. The first complete mitochondrial genome from the family Solasteridae, *Crossaster papposus* (Echinodermata, Asteroidea). *Mitochondrial DNA Part B* **2021**, *6*, 45–47. [[CrossRef](#)] [[PubMed](#)]
36. Zhang, D.; Gao, F.; Jakovčić, I.; Zou, H.; Zhang, J.; Li, W.X.; Wang, G.T. PhyloSuite: An integrated and scalable desktop platform for streamlined molecular sequence data management and evolutionary phylogenetics studies. *Mol. Ecol. Resour.* **2020**, *20*, 348–355. [[CrossRef](#)] [[PubMed](#)]
37. Duret, L. Evolution of synonymous codon usage in metazoans. *Curr. Opin. Genet. Dev.* **2002**, *12*, 640–649. [[CrossRef](#)] [[PubMed](#)]
38. Parvathy, S.T.; Udayasuriyan, V.; Bhadana, V. Codon usage bias. *Mol. Biol. Rep.* **2022**, *49*, 539–565. [[CrossRef](#)] [[PubMed](#)]
39. Perna, N.T.; Kocher, T.D. Patterns of nucleotide composition at fourfold degenerate sites of animal mitochondrial genomes. *J. Mol. Evol.* **1995**, *41*, 353–358. [[CrossRef](#)] [[PubMed](#)]
40. Bernt, M.; Merkle, D.; Ramsch, K.; Fritzsche, G.; Perseke, M.; Bernhard, D.; Schlegel, M.; Stadler, P.F.; Middendorf, M. CREx: Inferring genomic rearrangements based on common intervals. *Bioinformatics* **2007**, *23*, 2957–2958. [[CrossRef](#)]
41. Katoh, K.; Standley, D.M. MAFFT multiple sequence alignment software version 7: Improvements in performance and usability. *Mol. Biol. Evol.* **2013**, *30*, 772–780. [[CrossRef](#)]
42. Ranwez, V.; Douzery, E.J.; Cambon, C.; Chantret, N.; Delsuc, F. MACSE v2: Toolkit for the alignment of coding sequences accounting for frameshifts and stop codons. *Mol. Biol. Evol.* **2018**, *35*, 2582–2584. [[CrossRef](#)]
43. Castresana, J. Selection of conserved blocks from multiple alignments for their use in phylogenetic analysis. *Mol. Biol. Evol.* **2000**, *17*, 540–552. [[CrossRef](#)]
44. Talavera, G.; Castresana, J. Improvement of phylogenies after removing divergent and ambiguously aligned blocks from protein sequence alignments. *Syst. Biol.* **2007**, *56*, 564–577. [[CrossRef](#)]
45. Kalyaanamoorthy, S.; Minh, B.Q.; Wong, T.K.; Von Haeseler, A.; Jermini, L.S. ModelFinder: Fast model selection for accurate phylogenetic estimates. *Nat. Methods* **2017**, *14*, 587–589. [[CrossRef](#)] [[PubMed](#)]
46. Ronquist, F.; Teslenko, M.; Van Der Mark, P.; Ayres, D.L.; Darling, A.; Höhna, S.; Larget, B.; Liu, L.; Suchard, M.A.; Huelsenbeck, J.P. MrBayes 3.2: Efficient Bayesian phylogenetic inference and model choice across a large model space. *Syst. Biol.* **2012**, *61*, 539–542. [[CrossRef](#)] [[PubMed](#)]
47. Minh, B.Q.; Schmidt, H.A.; Chernomor, O.; Schrempf, D.; Woodhams, M.D.; Von Haeseler, A.; Lanfear, R. IQ-TREE 2: New models and efficient methods for phylogenetic inference in the genomic era. *Mol. Biol. Evol.* **2020**, *37*, 1530–1534. [[CrossRef](#)] [[PubMed](#)]
48. Letunic, I.; Bork, P. Interactive Tree Of Life (iTOL) v5: An online tool for phylogenetic tree display and annotation. *Nucleic Acids Res.* **2021**, *49*, W293–W296. [[CrossRef](#)] [[PubMed](#)]
49. Yang, Z. PAML 4: Phylogenetic analysis by maximum likelihood. *Mol. Biol. Evol.* **2007**, *24*, 1586–1591. [[CrossRef](#)] [[PubMed](#)]



50. Yang, Z.; Bielawski, J.P. Statistical methods for detecting molecular adaptation. *Trends Ecol. Evol.* **2000**, *15*, 496–503. [[CrossRef](#)] [[PubMed](#)]
51. Aylward, F. *Introduction to Calculating dN/dS Ratios with Codeml V. 2*; Virginia Tech: Blacksburg, VI, USA, 2018.
52. Yang, Z.; Wong, W.S.; Nielsen, R. Bayes empirical Bayes inference of amino acid sites under positive selection. *Mol. Biol. Evol.* **2005**, *22*, 1107–1118. [[CrossRef](#)]
53. Waterhouse, A.; Bertoni, M.; Bienert, S.; Studer, G.; Tauriello, G.; Gumienny, R.; Heer, F.T.; de Beer, T.A.P.; Rempfer, C.; Bordoli, L. SWISS-MODEL: Homology modelling of protein structures and complexes. *Nucleic Acids Res.* **2018**, *46*, W296–W303. [[CrossRef](#)]
54. Kopp, J.; Schwede, T. The SWISS-MODEL Repository of annotated three-dimensional protein structure homology models. *Nucleic Acids Res.* **2004**, *32*, D230–D234. [[CrossRef](#)]
55. Bienert, S.; Waterhouse, A.; De Beer, T.A.; Tauriello, G.; Studer, G.; Bordoli, L.; Schwede, T. The SWISS-MODEL Repository—New features and functionality. *Nucleic Acids Res.* **2017**, *45*, D313–D319. [[CrossRef](#)] [[PubMed](#)]
56. Moberly, J.G.; Bernards, M.T.; Waynant, K.V. Key features and updates for origin 2018. *J. Cheminformatics* **2018**, *10*, 1–2. [[CrossRef](#)] [[PubMed](#)]
57. Ballard, J.W.O.; Pichaud, N. Mitochondrial DNA: More than an evolutionary bystander. *Funct. Ecol.* **2014**, *28*, 218–231. [[CrossRef](#)]
58. Frank, A.; Lobry, J. Asymmetric substitution patterns: A review of possible underlying mutational or selective mechanisms. *Gene* **1999**, *238*, 65–77. [[CrossRef](#)] [[PubMed](#)]
59. Tanaka, M.; Ozawa, T. Strand asymmetry in human mitochondrial DNA mutations. *Genomics* **1994**, *22*, 327–335. [[CrossRef](#)]
60. Donath, A.; Jühling, F.; Al-Arab, M.; Bernhart, S.H.; Reinhardt, F.; Stadler, P.F.; Middendorf, M.; Bernt, M. Improved annotation of protein-coding genes boundaries in metazoan mitochondrial genomes. *Nucleic Acids Res.* **2019**, *47*, 10543–10552. [[CrossRef](#)] [[PubMed](#)]
61. Sun, X.-J.; Li, Q.; Kong, L.-F. Comparative mitochondrial genomics within sea cucumber (*Apostichopus japonicus*): Provide new insights into relationships among color variants. *Aquaculture* **2010**, *309*, 280–285. [[CrossRef](#)]
62. Perseke, M.; Fritzsche, G.; Ramsch, K.; Bernt, M.; Merkle, D.; Middendorf, M.; Bernhard, D.; Stadler, P.F.; Schlegel, M. Evolution of mitochondrial gene orders in echinoderms. *Mol. Phylogenetics Evol.* **2008**, *47*, 855–864. [[CrossRef](#)]
63. Jung, G.; Choi, H.-J.; Pae, S.; Lee, Y.-H. Complete mitochondrial genome of sea urchin: *Mesocentrotus nudus* (Strongylocentrotidae, Echinoidea). *Mitochondrial DNA* **2013**, *24*, 466–468. [[CrossRef](#)]
64. Dilly, G.; Gaitán-Espitia, J.; Hofmann, G. Characterization of the A antarctic sea urchin (*S terechinus neumayeri*) transcriptome and mitogenome: A molecular resource for phylogenetics, ecophysiology and global change biology. *Mol. Ecol. Resour.* **2015**, *15*, 425–436. [[CrossRef](#)]
65. Sharp, P.M.; Emery, L.R.; Zeng, K. Forces that influence the evolution of codon bias. *Philos. Trans. R. Soc. B Biol. Sci.* **2010**, *365*, 1203–1212. [[CrossRef](#)]
66. Plotkin, J.B.; Kudla, G. Synonymous but not the same: The causes and consequences of codon bias. *Nat. Rev. Genet.* **2011**, *12*, 32–42. [[CrossRef](#)]
67. Reyes, A.; Gissi, C.; Pesole, G.; Saccone, C. Asymmetrical directional mutation pressure in the mitochondrial genome of mammals. *Mol. Biol. Evol.* **1998**, *15*, 957–966. [[CrossRef](#)]
68. Komar, A.A. The Yin and Yang of codon usage. *Hum. Mol. Genet.* **2016**, *25*, R77–R85. [[CrossRef](#)]
69. Rodnina, M.V. The ribosome in action: Tuning of translational efficiency and protein folding. *Protein Sci.* **2016**, *25*, 1390–1406. [[CrossRef](#)]
70. Downton, M.; Campbell, N.J. Intramitochondrial recombination—is it why some mitochondrial genes sleep around? *Trends Ecol. Evol.* **2001**, *16*, 269–271. [[CrossRef](#)] [[PubMed](#)]
71. Zhong, J.; Li, G.; Liu, Z.-Q.; Li, Q.-W.; Wang, Y.-Q. Gene rearrangement of mitochondrial genome in the vertebrate. *Acta Genet. Sin.* **2005**, *32*, 322–330. [[PubMed](#)]
72. Scouras, A.; Beckenbach, K.; Arndt, A.; Smith, M.J. Complete mitochondrial genome DNA sequence for two ophiuroids and a holothuroid: The utility of protein gene sequence and gene maps in the analyses of deep deuterostome phylogeny. *Mol. Phylogenetics Evol.* **2004**, *31*, 50–65. [[CrossRef](#)] [[PubMed](#)]
73. Lin, M.-F.; Kitahara, M.V.; Luo, H.; Tracey, D.; Geller, J.; Fukami, H.; Miller, D.J.; Chen, C.A. Mitochondrial genome rearrangements in the Scleractinia/Corallimorpharia complex: Implications for coral phylogeny. *Genome Biol. Evol.* **2014**, *6*, 1086–1095. [[CrossRef](#)]
74. Quattrini, A.M.; Rodríguez, E.; Faircloth, B.C.; Cowman, P.F.; Brugler, M.R.; Farfan, G.A.; Hellberg, M.E.; Kitahara, M.V.; Morrison, C.L.; Paz-García, D.A. Palaeoclimate ocean conditions shaped the evolution of corals and their skeletons through deep time. *Nat. Ecol. Evol.* **2020**, *4*, 1531–1538. [[CrossRef](#)]
75. Quek, Z.B.R.; Chang, J.J.M.; Ip, Y.C.A.; Chan, Y.K.S.; Huang, D. Mitogenomes reveal alternative initiation codons and lineage-specific gene order conservation in echinoderms. *Mol. Biol. Evol.* **2021**, *38*, 981–985. [[CrossRef](#)]
76. Taylor, K.H.; Rouse, G.W.; Messing, C.G. Phylogeny and taxonomy of Himerometroidea (Echinodermata: Crinoidea). *Zootaxa* **2023**, *5277*, 149–164. [[CrossRef](#)] [[PubMed](#)]
77. Padial, J.M.; Miralles, A.; De la Riva, I.; Vences, M. The integrative future of taxonomy. *Front. Zool.* **2010**, *7*, 1–14. [[CrossRef](#)] [[PubMed](#)]
78. Pante, E.; Schoelincq, C.; Puillandre, N. From integrative taxonomy to species description: One step beyond. *Syst. Biol.* **2015**, *64*, 152–160. [[CrossRef](#)] [[PubMed](#)]

79. Rubinoff, D.; Cameron, S.; Will, K. A genomic perspective on the shortcomings of mitochondrial DNA for “barcoding” identification. *J. Hered.* **2006**, *97*, 581–594. [[CrossRef](#)] [[PubMed](#)]
80. Nielsen, R. Molecular signatures of natural selection. *Annu. Rev. Genet.* **2005**, *39*, 197–218. [[CrossRef](#)] [[PubMed](#)]
81. Castellana, S.; Vicario, S.; Saccone, C. Evolutionary patterns of the mitochondrial genome in Metazoa: Exploring the role of mutation and selection in mitochondrial protein-coding genes. *Genome Biol. Evol.* **2011**, *3*, 1067–1079. [[CrossRef](#)]
82. Bigham, A.W.; Mao, X.; Mei, R.; Brutsaert, T.; Wilson, M.J.; Julian, C.G.; Parra, E.J.; Akey, J.M.; Moore, L.G.; Shriver, M.D. Identifying positive selection candidate loci for high-altitude adaptation in Andean populations. *Hum. Genom.* **2009**, *4*, 1–12. [[CrossRef](#)]
83. Yang, Z.; Nielsen, R.; Goldman, N.; Pedersen, A.-M.K. Codon-substitution models for heterogeneous selection pressure at amino acid sites. *Genetics* **2000**, *155*, 431–449. [[CrossRef](#)]
84. Kimura, M. *The Neutral Theory of Molecular Evolution*; Cambridge University Press: Cambridge, UK, 1983.
85. Gillespie, J.H. *The Causes of Molecular Evolution*; Oxford University Press: Oxford, UK, 1991.
86. Ohta, T. The nearly neutral theory of molecular evolution. *Annu. Rev. Ecol. Syst.* **1992**, *23*, 263–286. [[CrossRef](#)]
87. Oliveira, D.C.; Raychoudhury, R.; Lavrov, D.V.; Werren, J.H. Rapidly evolving mitochondrial genome and directional selection in mitochondrial genes in the parasitic wasp *Nasonia* (Hymenoptera: Pteromalidae). *Mol. Biol. Evol.* **2008**, *25*, 2167–2180. [[CrossRef](#)]
88. Śmietanka, B.; Burzyński, A.; Wenne, R. Comparative genomics of marine mussels (*Mytilus* spp.) gender associated mtDNA: Rapidly evolving atp8. *J. Mol. Evol.* **2010**, *71*, 385–400. [[CrossRef](#)] [[PubMed](#)]
89. Sibley, C. *Phylogeny and Classification of the Birds: A Study in Molecular Evolution*; Yale University Press: New Haven, CT, USA, 1991.
90. Trumpower, B. The protonmotive Q cycle. Energy transduction by coupling of infarction: The BOOST randomised controlled clinical trial. *Lancet* **1990**, *364*, 9429.
91. Wirth, C.; Brandt, U.; Hunte, C.; Zickermann, V. Structure and function of mitochondrial complex I. *Biochim. Et Biophys. Acta (BBA)-Bioenerg.* **2016**, *1857*, 902–914. [[CrossRef](#)] [[PubMed](#)]
92. Mathiesen, C.; Hägerhäll, C. Transmembrane topology of the NuoL, M and N subunits of NADH: Quinone oxidoreductase and their homologues among membrane-bound hydrogenases and bona fide antiporters. *Biochim. Et Biophys. Acta (BBA)-Bioenerg.* **2002**, *1556*, 121–132. [[CrossRef](#)]
93. Da Fonseca, R.R.; Johnson, W.E.; O’Brien, S.J.; Ramos, M.J.; Antunes, A. The adaptive evolution of the mammalian mitochondrial genome. *BMC Genom.* **2008**, *9*, 1–22. [[CrossRef](#)] [[PubMed](#)]
94. Sanders, H.L.; Hessler, R.R. Ecology of the Deep-Sea Benthos: More detailed recent sampling has altered our concepts about the animals living on the deep-ocean floor. *Science* **1969**, *163*, 1419–1424. [[CrossRef](#)] [[PubMed](#)]
95. Ramos, N.I.; DeLeo, D.M.; Horowitz, J.; McFadden, C.S.; Quattrini, A.M. Selection in coral mitogenomes, with insights into adaptations in the deep sea. *Sci. Rep.* **2023**, *13*, 6016. [[CrossRef](#)]
96. Sha, Z.; Xiao, N. The first two complete mitogenomes of the order Apodida from deep-sea chemoautotrophic environments: New insights into the gene rearrangement, origin and evolution of the deep-sea sea cucumbers. *Comp. Biochem. Physiol. Part D Genom. Proteom.* **2021**, *39*, 100839.
97. Zhang, K.; Sun, J.; Xu, T.; Qiu, J.-W.; Qian, P.-Y. Phylogenetic relationships and adaptation in deep-sea mussels: Insights from mitochondrial genomes. *Int. J. Mol. Sci.* **2021**, *22*, 1900. [[CrossRef](#)] [[PubMed](#)]
98. Mu, W.; Liu, J.; Zhang, H. The first complete mitochondrial genome of the Mariana Trench *Freyastera benthophila* (Asteroidea: Brisingida: Brisingidae) allows insights into the deep-sea adaptive evolution of Brisingida. *Ecol. Evol.* **2018**, *8*, 10673–10686. [[CrossRef](#)] [[PubMed](#)]

**Disclaimer/Publisher’s Note:** The statements, opinions and data contained in all publications are solely those of the individual author(s) and contributor(s) and not of MDPI and/or the editor(s). MDPI and/or the editor(s) disclaim responsibility for any injury to people or property resulting from any ideas, methods, instructions or products referred to in the content.